EUROFUSION WPJET1-PR(14) 12688

F Romanelli et al.

Overview of the JET results

Preprint of Paper to be submitted for publication in Nuclear Fusion

This work has been carried out within the framework of the EUROfusion Consortium and has received funding from the Euratom research and training programme 2014-2018 under grant agreement No 633053. The views and opinions expressed herein do not necessarily reflect those of the European Commission.

Overview of the JET Results

F. Romanelli,
on behalf of JET contributors*

EUROfusion, JET, Culham Science Centre, OX14 3DB, Abingdon, UK

** See the Appendix of F. Romanelli et al.,*
Proceedings of the 25th IAEA Fusion Energy Conference 2014, Saint Petersburg, Russia

Preprint of Paper to be submitted for publication in
Nuclear Fusion

ABSTRACT

The JET programme focused on the consolidation of ITER design choices and the preparation for ITER operation, with a specific emphasis given to the Bulk Tungsten Melt Experiment that has been crucial for the final decision on the material choice for the day-one tungsten divertor in ITER. Integrated scenarios have been progressed with the reestablishment of long-pulse, high-confinement H-modes by optimizing the magnetic configuration and the use of ICRH to avoid tungsten impurity accumulation. Stationary discharges with detached divertor conditions and small Edge Localized Modes have been demonstrated by nitrogen seeding. The differences in confinement and pedestal behaviour before and after the ITER like Wall installation have been better characterized towards the development of high fusion yield scenarios in DT. Post-mortem analyses of the plasma facing components have confirmed the previously reported low fuel retention obtained by gas balance and shown that the pattern of deposition within the divertor has changed significantly with respect to the JET carbon wall campaigns due to the absence of thermally-activated chemical erosion of beryllium in contrast with carbon. Transport to remote areas is almost absent and two orders of magnitude less material is found in the divertor.

1. INTRODUCTION

The European fusion programme is moving into the phase of implementation of its Roadmap [1] that foresees the use of JET in Horizon 2020 as the main risk-mitigation element for the preparation of ITER operation. In 2004 the JET programme in support of ITER was launched consisting in three main elements [2]: (i) the installation of an ITER-like wall (ILW) to reproduce the same material mix for the plasma facing components of the nuclear phase of ITER; (ii) the development of plasma regimes of operation in the same configuration of ITER; and, (iii) a deuterium-tritium experiment to test the integrated regimes with the same fuel mix of ITER. During the last couple of years, the ILW characterization has been almost completed, significant progress has been made on the scenario development and the preparation of the DT campaign has started.

In 2013 and 2014, JET carried out experimental campaigns in deuterium at plasma currents I_p up to 4MA, magnetic field B_t up to 3.7T and auxiliary power up to P_{NBI}~27MW, P_{ICRH}~7MW, P_{LHCD}~3MW. The upgraded components of the neutral beam system (the newly configured sources, the actively cooled ducts and the high voltage power supplies (HVPS)) have all separately achieved the design targets. However, some problem with the old HVPS equipment and a major water leak on one octant at the end of 2013 have prevented the achievement of the maximum neutral beam power needed for a full scenario optimization with the ILW at plasma currents beyond 2.5MA. Nevertheless, after three years of operation with ILW (referred to in the following as the JET-ILW configuration) the JET heating systems have improved the performance achieved with the carbon wall (the JET-C configuration). The JET experience with the ILW shows the need of a careful preparation (as now integrated in the ITER research plan with the choice of the W divertor from the start of ITER operation) and a proper real-time protection system for the plasma facing components

in order to achieve continuous improvement in the plasma performance.

During this period, the ILW characterization has focused on the consolidation of the basis for the ITER decision on the first divertor [3], [4] with a specific emphasis given to the Bulk Tungsten Melt Experiment. For this purpose a divertor lamella has been misaligned in the most internal stack of the horizontal tile. A series of seven reproducible discharges produced shallow melting of tungsten and demonstrated the possibility of operating JET in these conditions without the occurrence of disruptions. The molten layer dynamics has been successfully modelled using the MEMOS code to validate the model and to allow a meaningful extrapolation to ITER. The results have been crucial for the final decision in favour of the tungsten divertor from the start of ITER operation.

In the first JET campaigns with the ILW [5], [6], [7] fuel retention and material migration studies had priority [8,9,10,11]. Now the focus of JET experiments has shifted towards integrated scenario development [12] to achieve low plasma-facing component (PFC) heat loads [13,14,15] and avoid tungsten accumulation [16] with the ultimate goal to achieve high performance plasmas [17,18] in view of the DT experiment. Magnetic geometry, strike point location and divertor pumping were established as key aspects for achieving good Hmode confinement, leading to the re-establishment of long pulse (~9s) high-confinement Hmodes at 2.5MA. This had to be combined with the control of tungsten accumulation by central heating using Ion Cyclotron Resonant Heating (ICRH) and sufficient gas fuelling. Significant effort was devoted to the use of impurity seeding [19] to produce core-divertor compatible scenarios which are essential for ITER, as well as high radiative scenarios which are required for DEMO. Stationary discharges have been produced by nitrogen seeding with fully detached divertor legs and small Edge Localized Modes (ELM). The use of N-seeding clearly increases the pedestal pressure but the global confinement is still 15% below the IPB98(y,2) scaling.

Comparisons between baseline and hybrid plasmas have blurred the distinction between the two scenarios, which now appear as a single operating domain. Dedicated power scans to elucidate the dependence on plasma beta of the energy confinement time have confirmed that on JET the power degradation is much weaker than the prediction of the IPB98(y,2) scaling.

Post-mortem analyses of the PFCs retrieved from the first ILW campaigns [20],[21],[22],[23],[24] have confirmed the previously reported low fuel retention obtained by gas balance, with the measured deuterium inventory below 0.25% of the injected amount of deuterium (a factor 16 below that for the carbon wall). These studies show that the reduced material erosion and migration lead to reduced trapping of fuel in deposited beryllium layers which incorporate less fuel in comparison with carbon layers. In addition, the pattern of deposition within the divertor has changed significantly with the ILW in comparison with the JET carbon wall [25] due to the lower level of re-erosion. Transport to remote areas is almost absent, with the only significant beryllium deposits (~15μm) found on the apron of the inner divertor. Overall, one order of magnitude lower deposition rate is found in the divertor compared to the carbon wall, with deposits in the floor of less than 2μm compared with more than 200μm thick deposits found after the last JET carbon-wall campaign due to long range migration via chemical erosion. These results are well reproduced by the WallDYN code. The

WallDYN extrapolation to ITER shows a reduction in the retention by more than a factor ten and implies that at least 3000 full power DT discharges could be produced on ITER before reaching the T-inventory limit. This is comparable with the time estimated to obtain a substantial erosion of the divertor.

The investigation of effective runaways mitigation methods has continued. Spontaneous generation of runaway electrons is not normally observed in JET-ILW. Runaways can be generated through massive Ar injection and accelerated up to 20MeV with the production of runaway currents up to 1.2MA. On JET, runaways can be suppressed by D_2 injection provided injection takes place before the thermal quench. Thereafter, runaway suppression using high-Z noble gases has been attempted but was found so far ineffective.

In section 2 we give an overview of all major results obtained with the ILW and the implications for ITER operation. In section 3 the development of ITER relevant scenarios in the new all-metal environment is presented, along with confinement and edge pedestal physics results. Conclusions and perspectives are presented in section 4.

2. OPERATION OF JET WITH THE ITER-LIKE WALL.

2.1 BULK TUNGSTEN MELT EXPERIMENT

A dedicated experiment has been carried out in JET to address the uncertainties associated with predicting the impact of transient tungsten melting in ITER due to ELMs [26,27,28,29]. The horizontal tile of the JET divertor is made by solid tungsten arranged in four stacks of lamellae in order to minimize the electromagnetic loads during disruptions (Fig.2). JET is the only tokamak able to produce repetitive ELMs with energy large enough (~300kJ per ELM) to melt tungsten. Deliberate shallow tungsten melting has been produced by operating with the outer strike point on one protruding lamella, intentionally modified and installed in one divertor module on the innermost stack as shown in Figure 2 [29]. A series of seven identical 3MA discharges with 23MW of heating power were produced. Within one second the base temperature of the lamella was raised to a value well below the melting temperature, but sufficiently high to facilitate the shallow melting by ELMs with power densities around $3GWm^{-2}$ during a further 0.5 second. The temperature on the top-side of the protruding and normal lamellae is measured by the two KL9 infrared diagnostics. The top view does not allow resolved measurements on the lamella side and makes the interpretation somewhat difficult. The temperature measurements are used as input for a 3D modelling of the heat transport through the lamella and the supporting structure. The results are consistent with melting by ELMs followed by re-solidification of tungsten in between events. The melting produced an enhanced tungsten source with occasional expulsion of small droplets (80-100μm) which did not significantly impact the main plasma and caused no disruptions during the experiments or thereafter. Almost 1mm depth (corresponding to a volume of ~6mm3) was moved/removed from the edge by up to several hundred ELMs during these pulses. The temperature of lamellae is shown in Figure 3 [30] for two pulses showing the temperature excursion caused by the ELMs. The analysis confirms that

transient melting during the ELMs occurs and not bulk melting due excessive tile temperatures. Most of the tungsten moved along the lamella edge although a precise mass balance will be possible only after post-mortem analysis. The propagation of molten material is consistent with a **j**×**B** driving force, where **j** is the current density into the surface (mainly due to thermo-electronic emission) and **B** is the local magnetic field [31]. Droplets on the lamella were seen to coalesce and grow, which increases the risk for longer pulse duration above the melt threshold. Nevertheless, the consequences of melting had no significant impact on JET operation.

The power load on the JET special lamella was substantially lower than expected. In order to match the IR measurements, the tungsten evaporation rate inferred from the WI 400.88nm line and the Planck radiation, the side heat loads must be reduced by a factor 2.5 in these Hmode discharges (a larger reduction factor of about five is needed to match the measurements in L-mode). The result is not yet understood: simulations including the gyro-radius smoothing effects predict only a 20% reduction [32], whereas the effect of vapour shielding turned out to be negligible for these conditions. Nevertheless, this finding has potentially positive implications for ITER, which may be less sensitive than previously feared to exposed edges created by chipping of mono-block edges or components outside tolerance. JET results are consistent with simulations of tungsten melting and propagation using the MEMOS code [33], which has been used to inform decisions on the choice of tungsten as the material for the first divertor in ITER. The results have also given confidence that flash melting of the tungsten divertor elements by ELMs is relatively benign compared to bulk melting as reported in other experiments [34].

2.2 MATERIAL EROSION AND MIGRATION, FUEL RECYCLING AND RETENTION

The JET ITER-Like Wall experiment provided for the first time the opportunity to explore the coupling between tokamak plasma operation and plasma-surface interaction in the beryllium/tungsten material environment of ITER, complementing earlier experiments in other divertor tokamaks with metallic walls like ASDEX Upgrade [35,36,37,38,39] and Alcator C-Mod [40],[41],[42]. These experiments are crucial in order to validate physics models and modelling tools for ITER with regard to material erosion and migration, fuel recycling and retention and impurity concentration and radiation.

The inter-connection of plasma-surface interaction with plasma-edge physics such as pedestal or divertor properties revealed that the impact of the first wall material on the plasma performance as well as the prominent role of chemical erosion of carbon was previously underestimated. The change in the material migration with the JET-ILW can be seen as one key result as it impacts directly or indirectly on the majority of plasma surface interaction processes mentioned above and contradicts partially the migration pattern predictions made in for beryllium/tungsten PFCs, which had assumed that physical spattering was dominant in the main chamber. In particular, it has been found that the primary beryllium source in JETILW is sputtering by low-energy (~10eV) ions in the main chamber resulting in a reduction by about a factor five of the eroded material with respect to

JET-C and in the lack of beryllium coverage of the inner divertor (intact tungsten surfaces remain). Furthermore, the virtual absence of chemical sputtering of beryllium inhibits the cycle of multiple erosion/deposition cycles within the divertor observed with carbon PFCs. Instead beryllium remains deposited at the positions where it lands after reflection or a physical sputtering process above the energetic threshold. It should be noted that, due to the low deposition rate, and the limited operational time on JET, the JET-ILW migration pattern could represent an intermediate state with respect to long-pulse operation. This is supported by the fact that two orders of magnitude less dust were recovered compared with the carbon wall.

A special effort was made to accurately quantify the reduction in long-term fuel retention with the JET-ILW, already measured in gas balance experiments, through post-mortem analysis. These results were used to validate the WallDYN code [43] and to allow a meaningful extrapolation to ITER. The code simulations reproduce both the reduction in fuel retention and the observed migration pattern. The remaining long-term retention is caused by implantation and co-deposition with beryllium and residual impurities. Short-term retention gained relative importance with respect to the low level of long-term retention and impacts on the recycling properties of both beryllium and tungsten and local plasma properties.

Predictions for ITER using WallDYN (Figure 4) [44], indicate that more than 3000 full power DT-discharges are possible before reaching the fuel-inventory limit, an amount comparable with that estimated for significant divertor erosion. If confirmed, the need of frequent fuel removal will be avoided.

2.3 DISRUPTIONS AND THE GENERATION OF RUNWAY ELECTRONS

Successful disruption mitigation [46],[47],[48] with massive gas injection of a mixture of argon and deuterium has been obtained and it is now mandatory for JET operation above 2MA. The radiation efficiency of massive gas injection using the Disruption Mitigation Valve on JET decreases in discharges with large thermal energy content. This behaviour is independent of the amount of injected impurities as long as the number of radiating atoms is above some limit. The radiated energy shows a clear toroidal asymmetry caused by a preexisting locked mode. This asymmetry changes phase when the mode is locked in a 90^{o} rotated toroidal position. Massive gas injection into X-point and O-point of the locked-mode island results in strong changes of the toroidal radiation distribution. Future experiments with two Disruption Mitigation Valves will attempt to minimize the radiation asymmetry.

Although after the installation of the ILW runaway electrons (RE) [49],[50] are rarely generated during spontaneous disruptions, they can be generated, as in the JET-C, using massive argon injection. Argon dominates the disruption plasma content, as shown in Figure 5 [51], thus decreasing the effect of the intrinsic impurities (carbon or beryllium) on the current quench dynamics. The conditions in which RE appear are similar between JET-C and JET-ILW: high toroidal field, high accelerating electric field and low densities (leading to lower critical electric field for RE generation) favour

large RE currents. They also show a strong dependence on plasma initial shape and vertical stability.

Runaway Electron energies were measured up to 20MeV for 200 to 380kA RE beams. RE beams up to 1.2MA at $I_p = 2$MA have been produced leading to substantial damage of tiles due to localized and toroidally asymmetrical melting on the inner wall and upper beryllium limiters [51]. It is to be noted that, within the uncertainty on the time reference of the IR camera, the interaction between the tile and the RE beam starts before the RE current decay, possibly due to the contact with the wall. After in-vessel visual inspection, the affected tile showed clear signs of melting and droplet ejection over an area of about $10cm^2$. RE suppression using massive high-Z gas injection was found to be ineffective so far for JET-ILW. However, early massive deuterium injection was found to be efficient provided that the gas reaches the plasma before the mixing phase of plasma and incoming gas, occurring at the thermal quench (Fig.6).

3. H-MODE PHYSICS IN AN ALL-METAL ENVIRONMENT

The qualification of the ELMy H-mode and of the hybrid regime with the ILW has provided a number of results of direct relevance for ITER. The baseline and hybrid scenario have been progressed towards ITER dimensionless parameters in plasmas up to 4MA, with Z_{eff} values as low as 1.1 and the domain of good confinement extended [53]. High performance scenarios are being successfully developed within the ILW constraints, namely the control of heat loads on the PFCs, the minimization of core tungsten concentration and the disruption mitigation/avoidance.

3.1 SCENARIO DEVELOPMENT AND OPTIMIZATION

H-mode and hybrid plasmas were obtained with energy confinement enhancement factors (H98) in the range of 0.9-1.2 [Joffrin] when compared with IPB98(y,2) scaling law [54]. It was previously reported that stationary H-modes could be re-established with the ILW by avoiding W-accumulation through the production of frequent ELMs regimes by gas puffing [12]. This, however, had a detrimental effect on confinement, possibly due to the pedestal cooling by gas injection. During the last two years stationary H-modes with confinement encompassing the ITER value ($H_{98} = 1$) have been produced by placing the divertor strike points such as to maximise pumping. In this way stationary, long pulse (~9s) H-modes have been produced at low value of Z_{eff} (Fig.7). Interestingly, confinement times in line or above the ITER98y2 scaling have been obtained also for values of the ratio P_{net}/P_{LH} between the power Pnet conducted through the separatrix and the LH threshold PLH in the range $1< P_{net}/P_{LH}<2$ (Fig.8).

Comparisons between baseline and hybrid plasmas in the range of $3\leq q_{95}\leq 4.3$ and $1\leq \beta_N \leq 2.7$, for the same values of the toroidal magnetic field (B_T), plasma current (I_p), density (n_e) and heating power (P_{NBI}) have blurred the distinction between the two scenarios, which now appear as a single operating domain. Small differences between the two scenarios remain: ion temperature profiles are more peaked and neutron rates are higher in the hybrid scenario. Power scans were performed under well-controlled conditions in the hybrid scenario in order to elucidate the validity of the power/beta

degradation included in the IPB98(y,2) scaling. The results confirmed earlier observations that the IPB98(y,2) scaling law is not consistent with the JET-ILW H-mode confinement time with respect to changes in the density (n_e) and heating power (P) ($\tau_{th,98y2} \propto n_e^{0.41} P^{-0.69}$) [55]. These experiments show a power degradation exponent as weak as –0.2 as shown in Figure 9 [56] and are consistent with previous observations of weak beta scaling of confinement in ELMy H-modes in DIII-D and JET, although this is less apparent in the full JET database. It should be noted that the JET-C high triangularity experiments were the only case, within this dedicated scan, to exhibit strong power degradation of confinement. It has been concluded [56] that these discharges are atypical of the confinement behaviour in JET in the controlled conditions of this experiment. This exceptional case appears to have been affected by variations in the neutral particle population in the main chamber, pointing out the role of neutral particles in plasma confinement. The stronger increase in plasma stored energy with power in the JET-ILW Hmode is associated with the increase in pedestal pressure and core pressure peaking and may be due to the interplay of different mechanisms: i) the temperature peaking increase is qualitatively consistent with previously proposed mechanisms relying on plasma rotation or supra-thermal ion pressure [57]; ii) the associated reduction in collisionality induces a density peaking as previously observed and consistent with theory [Angioni]; iii) the core plasma beta increase affects pedestal stability with the observed pedestal pressure increase consistent with peeling-ballooning paradigm.

JET-ILW experiments confirmed also the importance of central electron heating for achieving high performance H-modes in devices with high-Z PFCs. ICRH has proven to be capable of mitigating core tungsten accumulation, in agreement with the expectation of neoclassical theory [58] in high power H-modes (with total auxiliary heating power $P_{aux} > 20$MW) provided that the heating scenario is optimized and that the RF coupled power is high enough ($P_{RF} > 3$MW), as shown in figure 10 [59]. Distributed main chamber gas injection (as opposed to the divertor gas fuelling usually adopted) achieved the best RF coupling, due to the increase of the local density in front of the ICRH antennas [60,61]. The ICRF absorption and core electron heating were optimised by fine-tuning the resonance position and the minority hydrogen concentration. The best results were obtained with central ICRF power deposition ($r < 0.1$m) and with low ($n_H/n_e \sim 5\%$) minority concentrations, both guaranteeing an efficient collisional transfer of the absorbed power to the electrons. A minimum ICRF power is necessary for achieving sufficiently peaked temperature profiles in typical H-mode plasmas at central densities $n_{e0} = 7\text{-}9 \times 10^{19}/m^3$ for successful core impurity mitigation to take place. In most cases, however, lower levels (2–3MW) are sufficient for avoiding radiative collapse.

3.2 CORE-EDGE INTEGRATED SCENARIO DEVELOPMENT WITH IMPURITY SEEDING

Integration of plasma scenarios with tolerable PFC heat loads requires a significant fraction of the power to be radiated (frad>0.5). This is important for ITER and DEMO, the latter requiring frad> 90%, and may be also needed in full performance JET discharges with a long steady-state phase.

Using nitrogen seeding, radiative scenarios have been achieved with a stable radiated power fraction frad of 75%, full detached divertor conditions, electron temperatures below 5eV [Lowry]. In these conditions, tungsten concentrations are close to the detection limit and H-mode discharges up to 10 second have been produced, although at reduced confinement.

Nitrogen seeding has also been shown to increase the pedestal pressure by up to 40% in high triangularity and 15% in low triangularity plasmas restoring the confinement to a similar level to that seen with the carbon wall. Using N-seeding, stationary condition over 7s have been achieved on JET at 2.5MA/2.7T and 21MW input power with $\beta_N \sim 1.6$, $<n>/n_{GW} \sim 0.85$, $Z_{eff} \sim 1.6$, $f_{rad} \sim 55\%$, with low divertor target power loads and partial detachment between ELMs, as shown in Figure 11 [62]. These plasma performance are close to the desired ITER integrated plasma performance, in terms of Greenwald fraction, Z_{eff}, and divertor conditions, but the normalised energy confinement needs to be increased from $H_{98} \sim 0.85$ to $H_{98} = 1$ and the ELM energy losses need to be lowered from~4% to less than 1% of the pedestal stored energy. Seeded plasma with partially detached divertor, $H_{98} \sim 1$ and $\beta_N \sim 1.8$ will be a target of the next experimental campaign in which a higher level of input power should be available ($P_{aux} > 25$MW).

3.3 PROGRESS TOWARDS MAXIMUM FUSION PERFORMANCE

Hybrid scenarios at high β_N were further progressed towards lower collisionality values ($\nu^* \sim 0.04$), where better fusion performance is expected. In particular, a set of discharges with collisionalities low enough to match the upper range of the hybrid regimes in the JET carbon wall ($\nu^* \sim 0.04$) for low triangularity plasmas ($\delta \sim 0.15$) were achieved. These experiments used up to 25 MW of NBI auxiliary power with $I_P = 2$MA and $q_{95} = 3.8$ using a configuration with the strike point on the outer horizontal tile for maximising pumping, producing plasmas with H_{98} up to 1.4 and βN up to 3.4. Values of β_N up to 2.3 were achieved at $B_T = 2.9$T and $I_P = 2.5$MA leading to a new neutron rate record of 2.3×10^{16}/s for the ILW. The normalised confinement $H_{98} = 1.15$ is consistent with the findings of the beta scan experiment and on the basis of the observed dependence of H98 on β_N, is expected to achieve higher values if the target $\beta_N = 2.5$ could be reached. The β_N value so far achieved is only limited by the available heating power. The duration (up to 3s) of the high performance phase is limited by impurity accumulation and MHD occurring during the accumulation process, requiring further optimization of divertor plasma conditions while maximizing core fusion performance.

The extrapolation of these discharges to a 50/50 DT fuel mix predicts that about 15MW of fusion power could be produced. This target could be achieved in stationary conditions for about 5s, rather than transiently as in the 1997 JET DT experiment, corresponding to a total produced fusion energy of 75MJ, at 3.5MA/3.45T with 39MW of auxiliary power. These projections do not account for the contribution of the alpha particle heating and the beneficial isotope dependence of confinement, giving some margin in the achievable performance. In addition, recent analyses [Budny] of the 1997 record DT discharges show that core condition exceeding breakeven ($Q = 1$ with Q evaluated from the power balance inside mid radius) could have been already achieved in JET with core Q values

of about 1.5. Similarly, the extrapolated discharges are expected to achieve a higher core Q value than that inferred by the global analysis. However, the necessary increase of the radiated fraction to achieve divertor compatible conditions represents a major area of improvement for the next set of JET Campaigns.

3.4 L-H TRANSITION STUDIES

JET-ILW experiments show a minimum in the L-H threshold power as function of density, as seen on other machines and on JET-C with the MkII-GB divertor, and a reduction of the threshold by 30% in the high density branch. Both observations are potentially favourable for H-mode access on ITER [63],[64]. Nitrogen injection increases the threshold to JET-C values, suggesting that the difference between JET-C and JET-ILW can be accounted for by the impurity composition. Experiments indicate that the density at which the minimum occurs depends on both impurity content and divertor configuration and was not accessible in JET-C with the current divertor. Changes to the magnetic configuration in the divertor lead to changes in PL-H up to a factor 2. Fits of the edge density and temperature profiles show agreement with the assumption of a critical, diamagnetic driven, Er well (as proxy for the shearing rate) for each of the divertor configurations, but cannot explain the difference in PL-H between them. A transition that creates a strong inner-outer asymmetry in the divertor plasma conditions is observed with the same power scaling as the high density branch of the L-H threshold and precedes the L-H transition at high density. This transition depends on the divertor configuration and hints to changes in the scrape off layer directly affecting the transition.

3.5 PEDESTAL STUDIES WITH THE ILW

Pedestal studies have been carried out at JET with the main objective of addressing the physics responsible for the decrease in H-mode pedestal confinement observed in the initial phase of JET-ILW operation [65]. The effects of neutral recycling, plasma beta, plasma triangularity and nitrogen seeding on pedestal confinement and stability have been investigated, in the framework of the Peeling-Ballooning paradigm and making use of the EPED model [66]. It was found that low neutral recycling, achieved either by low deuterium gas injection rates or by divertor configurations with optimum pumping, and high-beta are necessary conditions for good pedestal (and core) confinement. Under such conditions the pedestals are consistent with the Peeling-Ballooning paradigm. In contrast, under conditions characterised by of high neutral recycling, additional physics is required in the pedestal model to explain the onset of the ELM instability. The physics mechanism leading to the increase in electron temperature in the pedestal with nitrogen seeding in high triangularity JET-ILW H-modes is not yet understood. The changes in the JET wall composition from CFC to beryllium/tungsten suggests the importance of the role of neutral recycling, low-Z impurities and scrape-off-layer physics in pedestal stability, elements that are not currently included in pedestal models. These aspects need to be addressed before a full predictive capability of the pedestal height can be achieved.

4 CONCLUSIONS AND PERSPECTIVES

Four years of JET operation with the ILW have provided sufficient confidence that the use of this combination of materials will not pose major problems for the successful operation of ITER. The low retention properties have been confirmed by the post mortem analysis and the melt layer experiment has shown that the consequence of melting can be tolerated for JET operation and that the JET results agree with the simulation codes that predict tolerable consequences also for ITER operation.

Significant progress has been made in expanding the domain in which good energy confinement is achieved by investigating magnetic configurations that allow a better pumping. Impurity seeding has been used to achieve steady regimes at high density and low Z_{eff} with detached divertor.

Overall JET demonstrated successful plasma operation in the beryllium/tungsten material combination, confirmed its advantageous behaviour with respect to material migration and fuel retention and provided a strong scientific basis for the ITER material selection. The ILW exploitation will continue in 2015 with the main aim of progressively increase the plasma performance. On the longer term, the preparation of a DT experiment is ongoing. The experiment is presently foreseen to take place in 2017 and according to the "Reference scenario" for the JET exploitation [1] will be followed by the machine being put in a safe state.

Following the completion of the feasibility studies for new JET enhancements, the design and R&D activity for a set of internal Resonant Magnetic Perturbation coils has been completed in collaboration with the Institute for Plasma Research in Gandhinagar. Its implementation on JET will require a decision on the "Alternative scenario" for the JET exploitation, consisting in the prolongation of JET up to 2022, tritium operation limited to a full-T experiment in 2017 and the DT experiment postponed to 2021.

ACKNOWLEDGMENTS

The author acknowledges the support of D. Borba, G. Sips, L. Horton and of the JET Task Force Leaders and Deputy Task Force Leaders for the preparation of the manuscript. This work was supported by EURATOM and carried out within the framework of the European Fusion Development Agreement. The views and opinions expressed herein do not necessarily reflect those of the European Commission.

REFERENCES

[1]. F. Romanelli et al. A roadmap to the realization of Fusion Energy (2012) ISBN 978-3-00-040720-8

[2]. J Pamela, et al. Journal of Nuclear Materials **363-365**, 1 – 11 (2007). "An ITER-like wall for JET" 10

[3]. R Pitts, et al. Journal of Nuclear Materials, Volume **415**, Issue 1, p. S957-S964. "Physics basis and design of the ITER plasma-facing components"

[4]. R.A. Pitts, et al Journal of Nuclear Materials, (438):S48, 2013 "A full tungsten divertor for

ITER: physics issues and design status."
[5]. G.F. Matthews et al 2011 Physica Scripta 2011 014001 " JET ITER-like wall—overview and experimental programme"
[6]. S. Brezinsek et al Journal of Nuclear Materials Volume **415**, Issue 1, Supplement, 1 August 2011, Pages S936–S942 "Overview of experimental preparation for the ITER-Like Wall at JET"
[7]. G.F. Matthews et al Journal of Nuclear Materials Volume **438**, Supplement, July 2013, Pages S2–S10 "Plasma operation with an all metal first-wall: Comparison of an ITER-like wall with a carbon wall in JET"
[8]. G.F. Matthews et al Physica Scripta 2014 2014 014015 "The second phase of JET operation with the ITERlike wall
[9]. S. Brezinsek, et al Nuclear Fusion, **53**(8):083023, 2013. " Fuel retention studies with the ITER-Like Wall in JET"
[10]. T. Loarer et al., "Comparison of fuel retention in JET between carbon and the ITER Like Wall", 20th International Conference on Plasma Surface Interactions in Controlled Fusion (Aachen, 2012)
[11]. V. Philipps et al., "Dynamic fuel retention and release under ITER like wall conditions in JET", 20th International Conference on Plasma Surface Interactions in Controlled Fusion (Aachen, 2012)
[12]. E. Joffrin et al 2014 Nuclear Fusion **54** 013011 " First scenario development with the JET new ITER-like wall"
[13]. C. Giroud et al 2012 Nuclear Fusion **52** 063022 "Integration of a radiative divertor for heat load control into JET high triangularity ELMy H-mode plasmas"
[14]. G Arnoux, et al Physica Scripta, 2014(**T159**):014009, 2014. "Power handling of the JET ITER-like wall."
[15]. G. Arnoux, et al Review of Scientific Instruments, **83**(10), 2012. "A protection system for the JET ITERlike wall based on imaging diagnostics"
[16]. A. Järvinen et al Journal of Nuclear Materials 2013 "Simulations of tungsten transport in the edge of JET ELMy H-mode plasmas"
[17]. G.P. Maddison et al Nuclear Fusion 2014 **54** 073016 "Contrasting H-mode behaviour with deuterium fuelling and nitrogen seeding in the all-carbon and metallic versions of JET"
[18]. M.N.A. Beurskens et al Nuclear Fusion 2014 **54** 043001 "Global and pedestal confinement in JET with a Be/W metallic wall"
[19]. C. Giroud et al Nuclear Fusion 2013 **53** 113025 "Impact of nitrogen seeding on confinement and power load control of a high-triangularity JET ELMy H-mode plasma with a metal wall"
[20]. G van Rooij et al., "Tungsten Divertor Erosion in all Metal Devices: Lessons from the ITER-LikeWall of JET and the all-W ASDEX Upgrade", 20th International Conference on Plasma Surface Interactions in Controlled Fusion (Aachen, 2012)

[21]. G.J. van Rooij et al Journal of Nuclear Materials 2013 “Tungsten divertor erosion in all metal devices: lessons from the ITER Like Wall of JET”
[22]. J Likonen et al Physica Scripta 2014 2014 014016 “ First results and surface analysis strategy for plasmafacing components after JET operation with the ITER-like wall”
[23]. K Heinola et al Physica Scripta 2014 2014 014013 “Tile profiling analysis of samples from the JET ITERlike wall and carbon wall”
[24]. J P Coad et al Physica Scripta 2014 2014 014012 “ Surface analysis of tiles and samples exposed to the first JET campaigns with the ITER-like wall”
[25]. A Widdowson et al 2014 Physica Scripta 2014 “Material migration patterns and overview of first surface analysis of the JET ITER-like wall”
[26]. J.W. Coenen, et al Nuclear Fusion, **53**(7):073043, 2013. “Long-term evolution of the impurity composition and impurity events with the ITER-like wall at JET.”
[27]. J.W. Coenen, et al Journal of Nuclear Materials, **438**:S27, 2013. “Evolution of surface melt damage, its influence on plasma performance and prospects of recovery.”
[28]. G Federici et al 2003 Plasma Physics and Controlled Fusion **45** 1523 “ Assessment of erosion of the ITER divertor targets during type I ELMs”
[29]. A Loarte et al Physica Scripta 2007 2007 222 “Transient heat loads in current fusion experiments, extrapolation to ITER and consequences for its operation”
[30]. J.W.Coenen et al Submitted to Nuclear Fusion “Type I ELM-induced transient melting in the JET W divertor”
[31]. Y. Corr, et al. PSI 2014 - submitted to Journal of Nuclear Materials, (P3-086), 2014. “Heat flux distribution and gyro-radius smoothing effect on misaligned CFC tile in the tore supra tokamak.”
[32]. R. Dejarnac et al. submitted to Nuclear Fusion, 2014. “PIC modeling of JET melt pulses with validated data.”
[33]. B. Bazylev, et al . Journal of Nuclear Materials, **390-391**:810-813, June 2009 “Experimental validation of 3d simulations of tungsten melt erosion under ITER-like transient loads”
[34]. J.W. Coenen et al.. PSI 2014 - submitted to Journal of Nuclear Materials, 2014. “ ELM induced tungsten melting and its impact on tokamak operation”
[35]. R Neu et al., Nuclear Fusion **45** (2005) 209 “Tungsten: an option for divertor and main chamber plasma facing components in future fusion devices”
[36]. R Neu et al 2007 Plasma Physics and Controlled Fusion **49** B59 “Plasma wall interaction and its implication in an all tungsten divertor tokamak”
[37]. O. Gruber et al 2009 Nuclear Fusion **49** 115014 “ Compatibility of ITER scenarios with full tungsten wall in ASDEX Upgrade”
[38]. R. Neu et al Journal of Nuclear Materials 2013 “Overview on plasma operation with a full tungsten wall in ASDEX Upgrade”
[39]. A C Sips and O Gruberfor the ASDEX Upgrade Team Plasma Physics and Controlled Fusion

2008 50 124028 “Compatibility of ITER scenarios with an all-W wall”
[40]. M. Greenwald et al 2005 Nucl. Fusion **45** S109 “ Overview of the Alcator C-Mod program”
[41]. B. Lipschultz et al., Journal of Nuclear Materials 363 (2007) 1110 “Influence of boronization on operation with high-Z plasma facing components in Alcator C-Mod”
[42]. B. Lipschultz et al Nuclear Fusion 2012 **52** 123002 “Divertor tungsten tile melting and its effect on core plasma performance”
[43]. K. Schmid et al., Journal of Nuclear Materials **415** (2011) S284 “An integrated model of impurity migration and wall composition dynamics for tokamaks”
[44]. S. Brezinsek et al., submitted for publication in Proceedings of the 21st International Conference on Plasma Surface Interactions, Kanazawa, Japan, 26th May 2014 - 30th May 2014 “ Plasma-surface interaction in the Be/W environment: conclusions drawn from the JET-ILW for ITER”
[45]. S. Brezinsek et al., Journal of Nuclear Materials **438** (2013) S303 “Residual carbon content in the initial ITER-Like Wall experiments at JET”
[46]. P. C. de Vries, et al., Plasma Physics and Controlled Fusion **54** (12) (2012) 124032. “The Impact of the ITER-Like Wall at JET on Disruptions”
[47]. M. Lehnen et al Journal of Nuclear Materials 2013 “Disruption heat loads and their mitigation in JET with the ITER-like wall”
[48]. M. Lehnen et al Nuclear Fusion 2013 **53** 093007 “Impact and mitigation of disruptions with the ITER-like wall in JET”
[49]. G. Papp et al Nuclear Fusion 2013 **53** 123017 “The effect of ITER-like wall on runaway electron generation in JET”
[50]. C. Reux et al submitted for publication in the Proceedings of the 25th IAEA Fusion Energy Conference, St Petersburg, Russia. “Runaway Electron Generation with the ITER-Like Wall and Efficiency of Massive Gas Injection at JET”
[51]. C. Reux et al submitted for publication in the Proceedings of the 21st International Conference on Plasma Surface Interactions, Kanazawa, Japan, 26th May 2014 - 30th May 2014 “Runaway Beam Studies During Disruptions at JET-ILW”
[52]. B. Bazylev, et al., Journal of Nuclear Materials **415** (1, Supplement) (2011) S841 – S844, “Modelling of Runaway Electron Beams for JET and ITER”
[53]. I. Nunes et al. this conference “Compatibility of high performance operation with JET ILW” [Joffrin]. E. Joffrin et al. this conference
[54]. ITER Physics Basis 1999 Nuclear Fusion **39** 2175
[55]. Beurskens M.N.A. et al 2013 Plasma Physics and Controlled Fusion **55** 124043 “ The effect of a metal wall on confinement in JET and ASDEX Upgrade”
[56]. C.D. Challis et al submitted to Nuclear Fusion Journal “Improved Confinement in JET High β Plasmas with an ITER-Like Wall”
[57]. Garcia et al. submitted for publication in the Proceedings of the 25th IAEA Fusion Energy

Conference, St Petersburg, Russia“ Core microturbulence and edge MHD interplay and stabilization by fast ions in tokamak confined plasmas”

[Angioni]. C. Angioni et al. Plasma Physics and Controlled Fusion **51** (2009) 124017 “Particle transport in tokamak plasmas, theory and experiment”

[58]. C. Angioni et al. Nucl. Fusion (2014) “Tungsten transport in JET H-mode plasmas in hybrid scenario, experimental observations and modelling”

[59]. E. Lerche et al submitted for publication in the Proceedings of the 25th IAEA Fusion Energy Conference, St Petersburg, Russia, “ICRH for mitigation of core impurity accumulation in JET-ILW”

[60]. D. Van Eester et al., Plasma Physics and Controlled Fusion **55** (2013) 025002 “ Ion cyclotron resonance heating-induced density modification near antennas”

[61]. D. Van Eester et al., Plasma Physics and Controlled Fusion **55** (2013) 055001 “Connection coefficients for cold plasma wave propagation near metallic surfaces”

[62]. C. Giroud et al, submitted to Nuclear Fusion Journal “Progress at JET in integrating ITER-relevant core and edge plasmas within the constraints of an ITER-like Wall”

[63]. E Delabie et al, submitted for publication in the Proceedings of the 25th IAEA Fusion Energy Conference, St Petersburg, Russia “Overview and Interpretation of L-H Threshold Experiments on JET with the ITER-like Wall”

[64]. C.F. Maggi et al, 2014 Nuclear Fusion **54** 023007 “L–H power threshold studies in JET with Be/W and C wall”

[65]. C.F. Maggi et al, submitted for publication in the Proceedings of the 25th IAEA Fusion Energy Conference, St Petersburg, Russia “Pedestal Confinement and Stability in JET-ILW ELMy H-mode Scenarios”

[66]. P.B Snyder, et al., Nuclear Fusion **51** (2011) 103016 “A first-principles predictive model of the pedestal height and width: development, testing and ITER optimization with the EPED model”

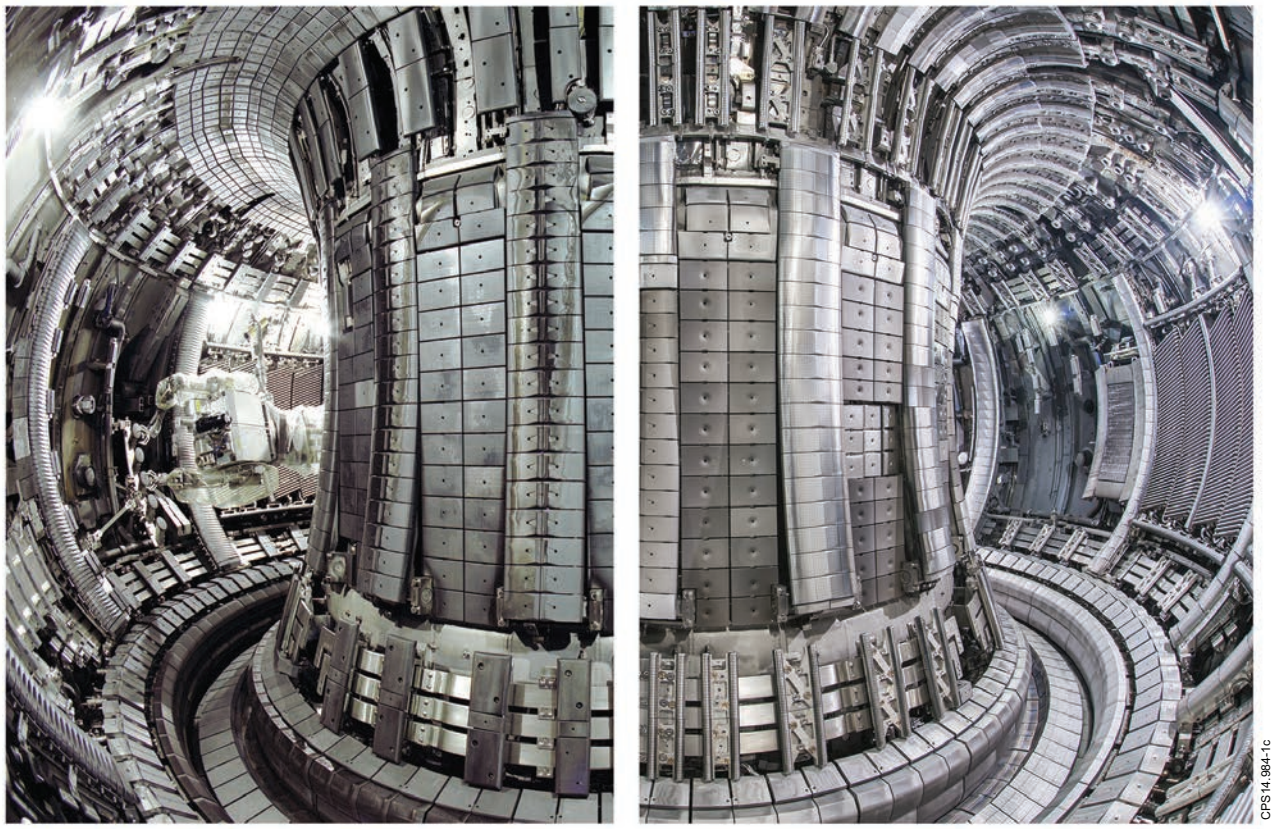

Figure 1:Picture of the interior of the JET vessel with an all carbon (JET-C) on the left and with the ITER-like wall (JET-ILW) with beryllium main chamber and tungsten divertor on the right.

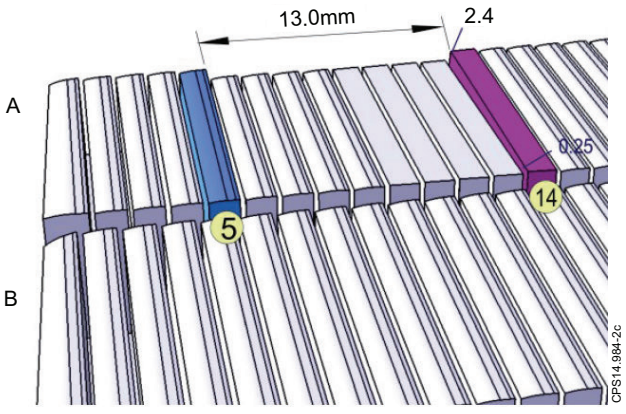

Figure 2: Schematic view of the lamella assembly in the modified stack.

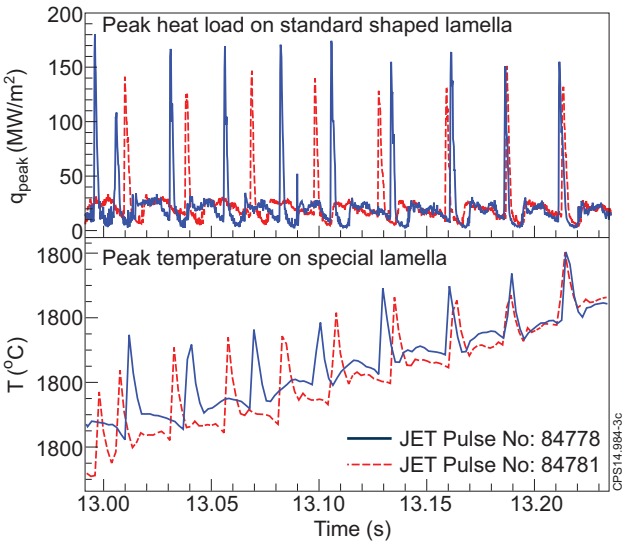

Figure 3: Temperature measurement for two pulses used in the experiment. Both shown for the reference and the special lamella.

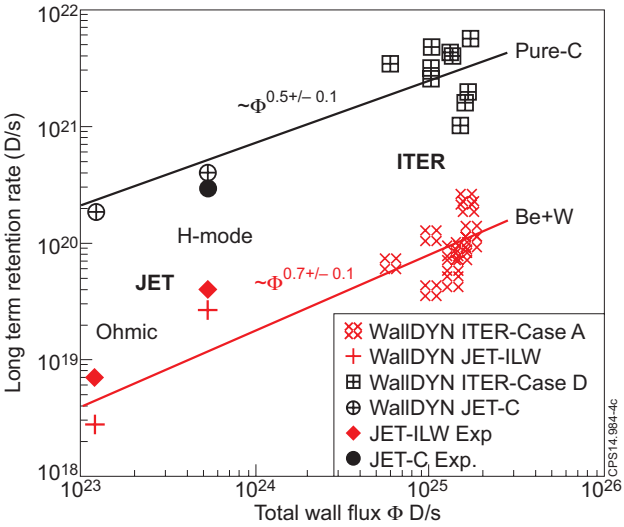

Figure 4: Long-term retention rate predictions for ITER made by WALLDYN [44].

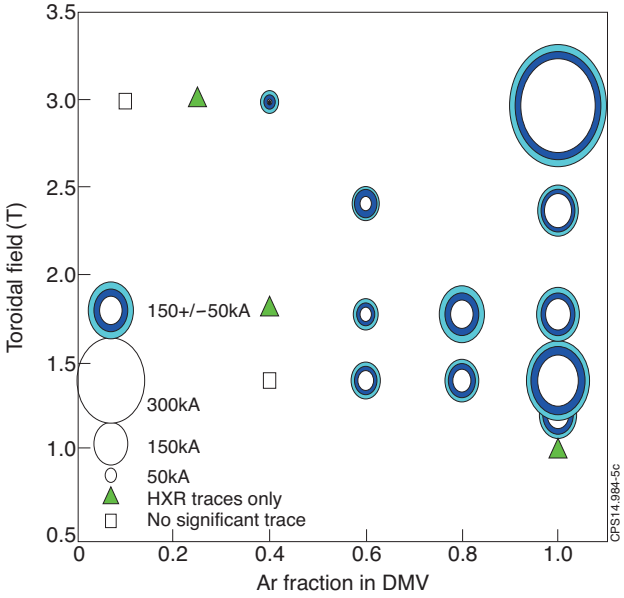

Figure 5: Operational domain for Runway Electron production in JET-ILW.

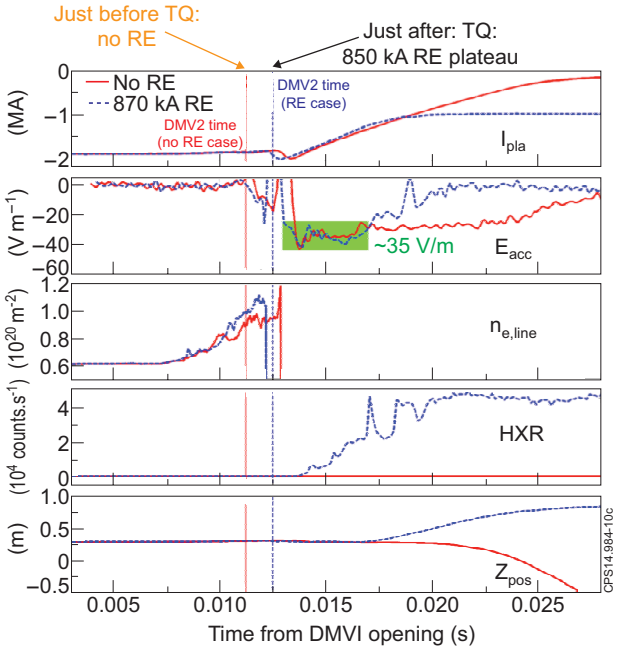

Figure 6: Runaway electrons suppression by D_2 massive injection. The injection is effective only if it takes place before the thermal quench (red). A delay of about 2ms in JET results in the production of a 850kA runaway beam.

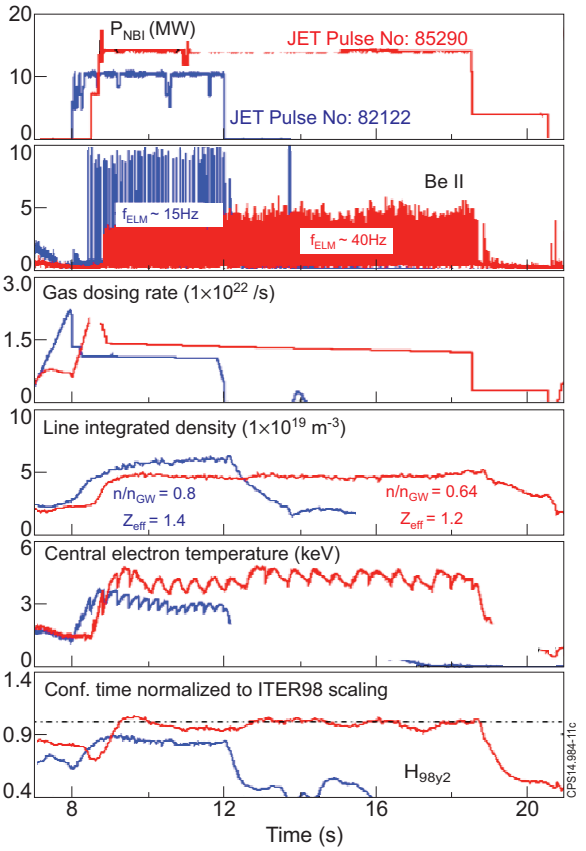

Figure 7: The optimization of the magnetic configuration led to the re-establishment of long-pulse, high-confinement H-modes (red). In blue the best discharge obtained in 2012 by controlled gas puffing to produce high-frequency ELMS and avoid W accumulation.

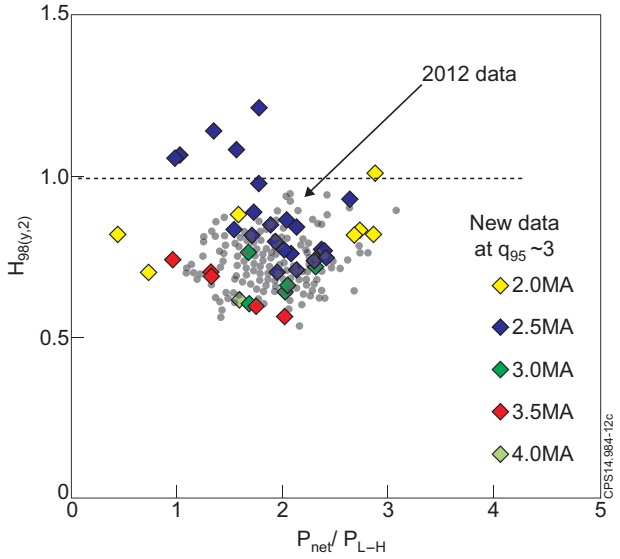

Figure 8: Achieved values of H_{98} as a function of the ratio between the power conducted through the magnetic separatrix and the L-H threshold power in the baseline scenario. The grey circles are the 2012 data. Diamonds are the results of the last two years. Optimization has been carried out so far only at 2.5MA.

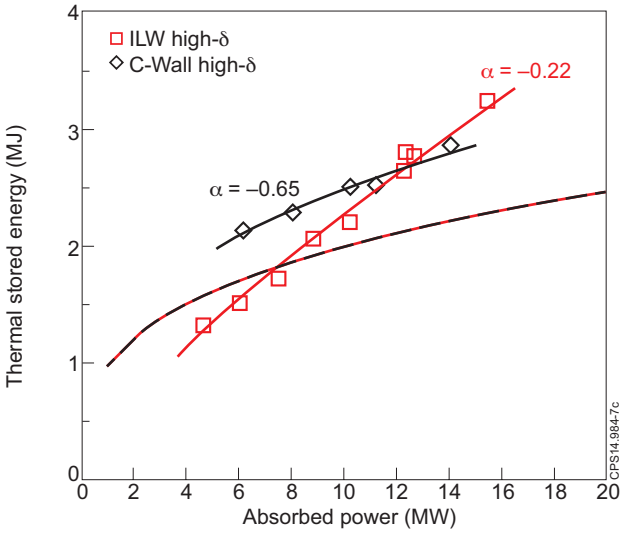

Figure 9: Plasma thermal stored energy as a function of absorbed heating power in the high triangularity configuration. The solid lines are fits to the data assuming a scaling of the form W_{th}~$P^{\alpha+1}$, where α is the exponent for the scaling for energy confinement time with power. The dashed lines represent the dependence using the IPB98(y,2) scaling (i.e. α = –0.69).

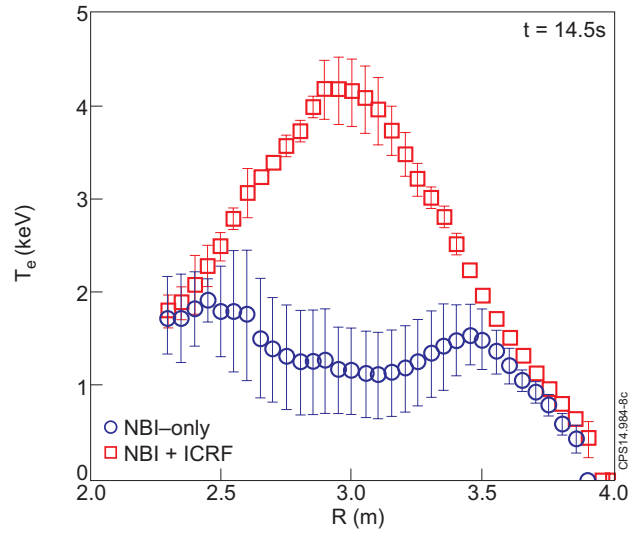

Figure 10: Comparison of the electron temperature profile at t = 14.5s from the LIDAR diagnostic of two similar nitrogen seeded discharges with NBI-only (JET Pulse No: 85413) and NBI+ICRF (JET Pulse No: 85412) with comparable total auxiliary power input.

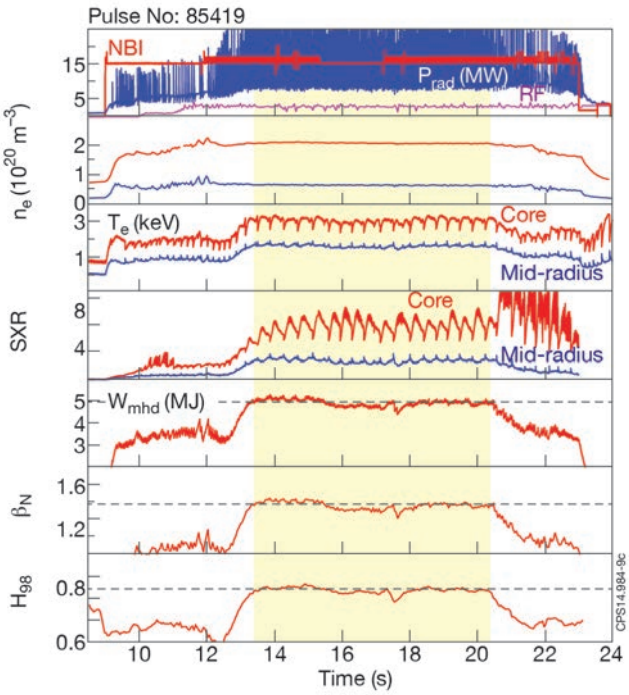

Figure 11: Time-traces for long nitrogen-seeded pulse JET Pulse No: 85419 at 2.5MA/2.7T showing avoidance of tungsten core accumulation in a high triangularity Nitrogen seeded plasma with VT divertor configuration by adding around 3MW of central ICRH heating power.

APPENDIX: LIST OF JET CONTRIBUTORS

M. Abhangi[34], P. Abreu[40], M. Aftanas[37], M. Afzal[3], K.M. Aggarwal[20], L. Aho-Mantila[94], E. Ahonen[1], M. Aints[90], M. Airila[94], R. Albanese[88], D. Alegre[46], E. Alessi[33], P. Aleynikov[42], A. Alfier[7], A. Alkseev[55], P. Allan[3], S. Almaviva[79], A. Alonso[46], B. Alper[3], I. Alsworth[3], D. Alves[40], G. Ambrosino[88], R. Ambrosino[89], V. Amosov[72], F. Andersson[11], E. Andersson Sundén[15], M. Angelone[74], A. Anghel[69], M. Anghel[68], C. Angioni[49], L. Appel[3], G. Apruzzese[74], P. Arena[21], M. Ariola[89], H. Arnichand[4], G. Arnoux[3], S. Arshad[30], A. Ash[3], E. Asp[15], O. Asunta[1], C.V. Atanasiu[69], Y. Austin[3], L. Avotina[87], M.D. Axton[3], C. Ayres[3], C. Bachmann[25], A. Baciero[46], D. Baião[40], V. Bailescu[71], B. Baiocchi[4], A. Baker[3], R.A. Baker3, I. Balboa[3], M. Balden[49], N. Balshaw[3], R. Bament[3], J.W. Banks[3], Y.F. Baranov[3], I.L. Barlow[3], M.A. Barnard[3], D. Barnes[3], R. Barnsley[42], A. Baron Wiechec[3], M. Baruzzo[7], V. Basiuk[4], M. Bassan[42], R. Bastow[3], A. Batista[40], P. Batistoni[74], R. Bauer[25], B. Bauvir[42], B. Bazylev[44], J. Beal[92], P.S. Beaumont[3], A. Becoulet[4], P. Bednarczyk[36], N. Bekris[26], M. Beldishevski[3], K. Bell[3], F. Belli[74], M. Bellinger[3], J.K. Belo[3], P. Belo[3,40], É. Belonohy[49], N.A. Benterman[3], H. Bergsåker[31], J. Bernardo[40], M. Bernert[49], M. Berry[3], L. Bertalot[42], M.N.A. Beurskens3, B. Bieg[36], J. Bielecki[36], T. Biewer[56], M. Bigi[7], P. Bílková[37], F. Binda[15], J.P.S. Bizarro[40], C. Björkas[85], K. Blackman[3], T.R. Blackman[3], P. Blanchard[23], E. Blanco[46], P. Blatchford[3], V. Bobkov[49], A. Boboc[3], G. Bodnár[95], O. Bogar[13], T. Bolzonella[7], L. Boncagni[74], R. Bonham[3], G. Bonheure[47], J. Boom[49], J. Booth[3], D. Borba[26,40], D. Borodin[29], A. Botrugno[74], C. Boulbe[45], P. Boulting[3], K.V. Bovert[29], M. Bowden[3], C. Bower[3], T. Boyce[3], H.J. Boyer[3], J.M.A. Bradshaw[3], V. Braic[70], B. Breizman[91], S. Bremond[4], P.D. Brennan[3], A. Brett[3], S. Brezinsek[29], M.D.J. Bright[3], M. Brix[3], W. Broeckx[60], M. Brombin[7], B.C. Brown[3], D.P.D. Brown[3], M. Brown[3], E. Bruno[42], J. Bucalossi[4], J. Buch[34], M.A. Buckley[3], K. Bucko[3], R. Budny[59], H. Bufferand[4], M. Bulman[3], N. Bulmer[3], P. Bunting[3], P. Buratti[74], G. Burcea[71], A. Burckhart[49], A. Buscarino[21], P.R. Butcher[3], N.K. Butler[3], I. Bykov[31], J. Byrne[3], A. Byszuk[36], A. Cackett[3], P. Cahyna[37], G. Cain[3], G. Calabrò[74], C.P. Callaghan[3], D.C. Campling[3], J. Cane[3], B. Cannas[12], A.J. Capel[3], M. Caputano[88], P.J. Card[3], A. Cardinali[74], P. Carman[3], D. Carralero[49], L. Carraro[7], B.B. Carvalho[40], I. Carvalho[40], P. Carvalho[40], F.J. Casson[3], C. Castaldo[74], R. Cavazzana[7], M. Cavinato[7], A. Cazzaniga[33], M. Cecconello[15], E. Cecil[59], A. Cenedese[7], C. Centioli[74], R. Cesario[74], C.D. Challis[3], M. Chandler[3], D. Chandra[34], C.S. Chang[59], A. Chankin[49], I.T. Chapman[3], S.C. Chapman[19], M. Chernyshova[36], P. Chiru[69], G. Chitarin[7], B. Chouli[4], N. Chung[3], G. Ciraolo[4], D. Ciric[3], J. Citrin[28], F. Clairet[4], E. Clark[3], D. Clatworthy[3], R. Clay[3], M. Clever[29], J.P. Coad[3 ,94], P.A. Coates[3], V. Coccorese[88], V. Cocilovo[74], S. Coda[23], R. Coelho[40], J.W. Coenen[29], I. Coffey[20], L. Colas[4], S. Collins[3], J.E. Conboy[3], S. Conroy[15], N. Cook[3], D. Coombs[3], D. Cooper[3], S.R. Cooper[3], Y. Corre[4], G. Corrigan[3], S. Cortes[40], D. Coster[49], A.S. Couchman[3], M. Cox[3], M.P. Cox[3], P. Cox[3], T. Craciunescu[69], S. Cramp[3], F. Crisanti[74], I. Cristescu[44], G. Croci[33], O. Croft[3], K. Crombé[10,47], R. Crowe[3], N. Cruz[40], G. Cseh[95], K. Cull[3], L. Cupido[40], D. Curran[80], M. Curuia[68], A. Czarnecka[36], T. Czarski[36], S. Dalley[3], A. Dalziel[3], D. Darrow[59], R. Davies[3], W. Davis[42,59], C. Day[44], I.E. Day[3], E. de la Cal[46], E. de la Luna[46], M. De Magistris[88], J. L. de Pablos[46], G. De Tommasi[88],

P.C. de Vries[28], K. Deakin[3], J. Deane[3], J. Decker[4], F. Degli Agostini[7], R. Dejarnac[37], E. Delabie[28], N. den Harder[28], R.O. Dendy[19], P. Denner[29], S. Devaux[49], P. Devynck[4], F. Di Maio[42], L. Di Pace[74], T. Dittmar[29], D. Dodt[49], T. Donné[25], P. Dooley[6], S.E. Dorling[3], S. Dormido-Canto[77], S. Doswon[3], D. Douai[4], P.T. Doyle[3], T. Dreischuh[35], P. Drewelow[50], V. Drozdov[3], K. Drozdowicz[36], R. Dumont[4], P. Dumortier[47], D. Dunai[95], M. Dunne[80], I. Ďuran[37], F. Durodié[47], P. Dutta[34], B. Duval[23], R. Dux[49], K. Dylst[60], N. Dzysiuk[15], P.V. Edappala[34], A.M. Edwards[3], Th. Eich[49], A. Ekedahl[4], T. Elevant[31], R. El-Jorf[3], C.G. Elsmore[3], G. Ericsson[15], A. Eriksson[11], J. Eriksson[15], L.G. Eriksson[27], B. Esposito[74], H.G. Esser[29], D. Esteve[4], G.E. Evans[3], J. Evans[3], G.D. Ewart[3], D.T. Ewers[3], D. Fagan[3], D. Falie[69], J.W. Farthing[3], A. Fasoli[23], L. Fattorini[33], B. Faugeras[45], J. Faustin[23], N. Fawlk[3], G. Federici[25], N. Fedorczak[4], R.C. Felton[3], C. Fenzi[4], A. Fernades[40], H. Fernandes[40], J. Ferreira[40], J.A. Fessey[3], L. Figini[33], A. Figueiredo[40], J. Figueiredo[26,40], A. Fil[4], P. Finburg[3], M. Firdaouss[4], U. Fischer[44], L. Fittill3, M. Fitzgerald[3], D. Flammini[74], J. Flanagan[3], C. Fleming[3], K. Flinders[3], A. Formisano[61], L. Forsythe[3], L. Fortuna[21], M. Fortune[3], M. Frasca[21], L. Frassinetti[31], M. Freisinger[29], R. Fresa[82], D. Frigione[74], V. Fuchs[37], J. Fyvie[3], M. Gadomska[25], K. Gál[26,49], C. Galperti[33], R. Galvão[5], X. Gao[38], S. Garavaglia[33], J. Garcia[4], A. Garcia- Carrasco[31], M. García-Munoz[49,76], M. Gardner[3], L. Garzotti[3], P. Gaudio[79], E. Gauthier[4], J.W. Gaze[3], D.F. Gear[3], S.J. Gee[3], M. Gelfusa[79], E. Genangeli[74], S. Gerasimov[3], G. Gervasini[33], M. Ghate[34], M. Gherendi[69], J.C. Giacalone[4], L. Giacomelli[81], C.S. Gibson[3], T. Giegerich[44], D. Gin[41], E. Giovannozzi[74], J.B. Girardo[4], C. Giroud[3], G. Giruzzi[4], C. Gleason-Gonzalez[44], J. Godwin[3], P. Gohil[32], A. Gójska[36], V. Goloborod'ko[86], R. Gomes[40], B. Gonçalves[40], M. Goniche[4], S. Gonzalez[25], B. Goodsell[3], A. Goodyear[3], G. Gorini[81], A. Goussarov[60], B. Graham[3], M.E. Graham[3], J. Graves[23], N. Grazier[3], N.R. Green[3], H. Greuner[49], E. Grigore[69], F.S. Griph[3], C. Grisolia[4], D. Grist[3], M. Groth[1], C.N. Grundy[3], M. Gryaznevich[66], D. Guard3, D. Gubb[3], C. Guillemaut[4], Y. Guo[29], H. H Utoh[43], L.J. Hackett[3], S. Hacquin[4], A. Hagar[3], A. Hakola[94], M. Halitovs[87], S.J. Hall[3], S.P. Hallworth Cook[3], K. Hammond[3], J. Hart3, D. Harting[3,29], N. Hartmann[29], T.D.V. Haupt[3], N.C. Hawkes[3], J. Hawkins[3], P.W. Haydon[3], S. Hazel[3], P.J.L. Heesterman[3], K. Heinola[85], C. Hellesen[15], T. Hellsten[31], W. Helou[4], O.N. Hemming[3], T.C. Hender[3], M. Henderson[42], R. Henriques[40], D. Hepple[3], G. Hermon[3], C. Hidalgo[46], E.G. Highcock[18], J.W. Hill[3], M. Hill[3], J. Hillairet[4], J. Hillesheim[3], D. Hillis[56], A. Hjalmarsson[15], J. Hobirk[49], C.H.A. Hogben[3], G.M.D. Hogeweij[28], D.A. Homfray[3], J. Horáček[37], A.R. Horton[3], L.D. Horton[27], S.P. Hotchin[3], M.R. Hough[3], P.J. Howarth[3], A. Huber[29], T.M. Huddleston[3], M. Hughes[3], C.L. Hunter[3], H. Hurzlmeier[25], S. Huygen[47], P. Huynh[4], J. Igitkhanov[44], D. Iglesias[3], M. Imríšek[37], D. Ivanova[31], I. Ivanova-Stanik[36], E. Ivings[3], S. Jachmich[26,47], A.S.Jacobsen[66], P. Jacquet[3], K. Jakubowska[36], J. James[3], F. Janky[37], A. Järvinen1, F. Jaulmes[28], S. Jednorog[36], C. Jenkins[3], I. Jenkins[3], K. Ješko[37], E. Joffrin[4], R. Johnson[3], T. Johnson[31], L. Joita[3], G. Jones[3], T.T.C. Jones[3], L. Joyce[3], C. Jupén[16], K. K Hoshino[43], A. Kallenbach[49], D. Kalupin[25], K. Kamiya[43], J. Kaniewski[3], A. Kantor[3], J. Karhunen1, G. Kasprowicz[36], G. Kaveney[3], Y. Kazakov[47], D.L. Keeling[3], J. Keep[3], M. Kempenaars[3], C. Kennedy[3], D. Kenny[3], E. Khilkevich[41], M. Kiisk[90], H-T. Kim[3], H.S. Kim[62], C. King[3], D. King[3],

R.F. King[3], D.J. Kinna[3], V. Kiptily[3], K. Kirov[3], A. Kirschner[29], G. Kizane[87], C. Klepper[56], M. Knaup[29], S.J. Knipe[3], T. Kobuchi[43], F. Köchl[93], G. Kocsis[95], D. Kogut4, S. Koivuranta[94], M. Köppen[29], T. Koskela[1], H.R. Koslowski[29], V. Kotov[29], E. Kowalska Strzęciwilk[36], A. Krasilnikov[72], V. Krasilnikov[72], A. Kreter[29], K. Krieger[49], Y. Krivchenkov[3], A. Krivska[47], U. Kruezi[3], I. Ksiazek[36], A. Kukushkin[55], A. Kundu[34], T. Kurki-Suonio[1], O.J. Kwon[8], V. Kyrytsya[47], M. Laan[90], C. Labate[6], L. Laguardia[33], N. Lam[3], C. Lane[3], P.T. Lang[49], J. Lapins[87], A. Lasa[85], J.R. Last[3], A. Lawson[3], K.D. Lawson[3], A. Lazaros[53], E. Lazzaro[33], S. Lee[52], H.J. Leggate[22], M. Lehnen[29,42], D. Leichtle[30], P. Leichuer[3], F. Leipold[42], I. Lengar[63], M. Lennholm[27], E. Lerche[47], M. Leyland[92], W. Leysen[60], Y. Liang[29], J. Likonen[94], V. Lindholm[1], J. Linke[29], Ch. Linsmeier[29], B. Lipschultz[51,92], X. Litaudon[4,26], G. Liu[42], Y. Liu[3,38], V.P. Lo Schiavo[88], T. Loarer[4], A. Loarte[42], R.C. Lobel[3], N. Lohr[44], P.J. Lomas[3], J. Lönnroth[1,26], J. López[46], J. M. López[78], F. Louche[47], A.B. Loving[3], S. Lowbridge[3], C. Lowry[27], T. Luce[32], R.M.A. Lucock[3], A. Lukin[57], A.M. Lungu[69], C.P. Lungu[69], I. Lupelli[3], A. Lyssoivan[47], P. Macheta[3], A.S. Mackenzie[3], G. Maddaluno[74], G.P. Maddison[3], B. Magesh[34], P. Maget[4], C.F. Maggi[49], H. Maier[49], J. Mailloux[3], A. Maj[36], T. Makkonen[1], R. Makwana[34], A. Malaquias[40], F. Mansffield[3], M. Mansfield[80], M.E. Manso[40], P. Mantica[33], M. Mantsinen[2], A. Manzanares[75], Y. Marandet[4], N. Marcenko[72], C. Marchetto[33], O. Marchuk[29], M. Marinelli[79], M. Marinucci[74], T. Markovič[37], D. Marocco[74], L. Marot[64], C.A. Marren[3], S. Marsen[50], R. Marshal[3], A. Martin[3], D.L. Martin[3], Y. Martin[23], A. Martín de Aguilera[46], J.R. Martín-Solís[9], A. Masiello[7], M. Maslov[3], V. Maslova[3], S. Matejcik[13], M. Mattei[61], G.F. Matthews[3], D. Matveev[10], M. Matveev[29], F. Maviglia[6,25], M. Mayer4[9], M-L. Mayoral[25], D. Mazon[4], C. Mazzotta[74], R. McAdams[3], P.J. McCarthy[80], K.G. McClements[3], K. McCormick[49], P.A. McCullen[3], D. McDonald[25], R. Mcgregor[3], R. McKean[3], J. McKehon[3], R. McKinley[3], I. Meadows[3], R.C. Meadows[3], F. Medina[46], M. Medland[3], S. Medley[3], S. Meigh[3], A.G. Meigs[3], L. Meneses[40], S. Menmuir[31], I.R. Merrigan[3], Ph. Mertens[29], S. Meshchaninov[72], A. Messiaen[47], B. Meszaros[25], H. Meyer[3], G. Miano[88], R. Michling[42], D. Middleton-Gear[3], J. Miettunen[1], P. Migliucci[79], E. Militello-Asp[3], S. Minucci[88], F. Mirizzi[74], Y. Miyoshi[43], J. Mlynář[37], I. Monakhov[3], P. Monier-Garbet[4], R. Mooney[3], S. Moradi[24], S. Mordijck[32], L. Moreira[3], R. Moreno[46], P.D. Morgan[3], R. Morgan[3], L. Morley[3], C. Morlock[25], A.W. Morris[3], J. Morris[3], L. Moser[64], D. Moulton[1], A. Murari[7], A. Muraro[33], I. Mustata[69], N.N Asakura[43], F. Nabais[40], T. Nakano[43], E. Nardon[4], V. Naulin[66], M.F.F. Nave[40], I. Nedzelski[40], N. Neethiraj[3], G. Nemtsev[72], F. Nespoli[23], A. Neto[30,40], R.Neu[49], O. Neubauer[29], M. Newman[3], K.J. Nicholls[3], D. Nicolai[29], T. Nicolas[4], P. Nieckchen[25], P. Nielsen[7], M.P.S. Nightingale[3], E. Nilsson[4], D. Nishijima[83], C. Noble[3], M. Nocente[81], D. Nodwell[3], H. Nordman[11], I. Nunes[40], B. O'Meara[3], M. Oberkofler[49], B. Obryk[36], T. Odupitan[3], M.T. Ogawa[43], T. O'Gorman[3], M. Okabayashi[59], S. Olariu[67], M. O'Mullane[14], J. Ongena[47], F. Orsitto[74], B.I. Oswuigwe[3], N. Pace[3], D. Pacella[74], A. Page[3], A. Paget[3], D. Pagett[3], E. Pajuste[87], S. Palazzo[21], J. Pamela[4], S. Pamela[4], A. Panin[29], S. Panja[34], P. Papp[13], V. Parail[3], P. Paris[90], S.C.W. Parish[3], M. Park[52], A. Parsloe[3], R. Pasqualotto[7], I.J. Pearson[3], M.A. Pedrosa[46], R. Pereira[40], E. Perelli Cippo[33],

Ch. Perez von Thun[49], C. Perez-Von-Thun[26], V. Pericoli-Ridolfini[74], A. Perona[58], S. Peruzzo[7], S. Peschanyi[44], M. Peterka[37], P. Petersson[31], G. Petravich[95], V. Petržilka[37], D. Pfefferle[23], V. Philipps[29], A. Pietropaolo[74], M. Pillon[74], G. Pintsuk[29], P. Piovesan[7], A. Pires dos Reis[39], A. Pironti[88], F. Pisano[12], R. Pitts[42], C. Plusczyk[44], V. Plyusnin[40], N. Pomaro[7], O. Pompilian[69], P.J. Pool[3], S. Popovichev[3], F. Porcelli[58], C. Porosnicu[69], M. Porton[3], A. Pospieszczyk[29], G. Possnert[15], S. Potzel[49], T. Powell[3], K. Pozniak[36,] J. Pozzi[3], V. Prajapati[34], R. Prakash[34], G. Prestopino[79], D. Price[3], R. Price[3], P. Prior[3], R. Prokopowicz[36], R. Proudfoot[3], P. Puglia[39], M.E. Puiatti[7], D. Pulley[3], K. Purahoo[3], Th. Pütterich[49], A. Quercia[88], E. Rachlew[17], M. Rack[29], J. Raeder[25], M.S.J. Rainford[3], G. Ramogida[74], S. Ranjan[34], J. Rasmussen[66], J.J. Rasmussen[66], K. Rathod[34], G. Rattá[46], C. Rayner[3], M. Rebai[33,81], D. Reece[3], A. Reed[3], D. Réfy[95], B. Regan[3], J. Regana[25], M. Reich[49], P. Reid[3], M. Reinelt[49], M.L. Reinke[92], M. Reinke[56], D. Reiser[29], D. Reiter[29], D. Rendell[3], C. Reux[4], V. Riccardo[3], F.G. Rimini[3], M. Riva[74], J.E.C. Roberts[3], R.J. Robins[3], S.A. Robinson[3], T. Robinson[3], D.W. Robson[3], P. Roddick[3], R. Rodionov[72], V. Rohde[49], F. Romanelli[74], M. Romanelli[3], S. Romanelli[3], A. Romano[74], D. Rowe[3], S. Rowe[3], A. Rowley[3], M. Rubel[31], G. Rubinacci[88], L. Ruchko[39], M. Ruiz[78], C. Ruset[69], L. Ryć[36], J. Rzadkiewicz[36], S. Saarelma[3], R. Sabot[4], S. Sadakov[29], E. Safi[85], P. Sagar[3], G. Saibene[30], F. Saint-Laurent[4], M. Salewski[66], A. Salmi[94], F. Salzedas[40], U. Samm[29], D. Sandiford[3], P. Sandquist[11], P. Santa[34], M.I.K. Santala[1], F. Sartori[30], R. Sartori[30], R. Saunders[3], O. Sauter[23], R. Scannell[3], A. Scarabosio[49], T. Schlummer[29], V. Schmidt[7], O. Schmitz[29], S. Schmuck[3,50], M. Schneider[4], M. Scholz[36], K. Schöpf[86], B. Schweer[29], G. Sergienko[29], A. Serikov[44], M. Sertoli[49], A. Shabbir[10], M. Shannon[25], M.M.J. Shannon[3], S.E. Sharapov[3], I. Shaw[3], S.R. Shaw[3], A. Shepherd[3], A. Shevelev[41], A. Shumack[28], M. Sibbald[3], B. Sieglin[49], C. Silva[40], P.A. Simmons[3], A. Sinha[34], S.K. Sipilä[1], A.C.C. Sips[27], P. Sirén[94], A. Sirinelli[42], H. Sjöstrand[15], M. Skiba[15], R. Skilton[3], B. Slade[3], N. Smith[3], P.G. Smith[3], T.J. Smith[3], L. Snoj[63], S. Soare[68], E.R. Solano[26,46], S. Soldatov[10], P. Sonato[7], A. Sopplesa[7], J. Sousa[40], C.B.C. Sowden[3], C. Sozzi[33], A. Sparkes[3], T. Spelzini[3], F. Spineanu[69], G. Stables[3], I. Stamatelatos[54], M.F. Stamp[3], V. Stancalie[69], R. Stankiewicz[36], G. Stankūnas[48], M. Stano[13], C. Stan-Sion[67], D.E. Starkey[3], M.J. Stead[3], M. Stejner[66], A.V. Stephen[3], M. Stephen[34], B.D. Stevens[3], D. Stoyanov[35], J. Strachan[59], P. Strand[11], M. Stransky[11], P. Ström[31], G. Stubbs[3], W. Studholme[3], F. Subba[58], H.P. Summers[14], Y. Sun[29], J. Svensson[50], N. Sykes[3], B.D. Syme[3], T. Szabolics[95], G. Szepesi[3,33], A. Szydlowski[36], T.T Suzuki[43], F. Tabarés[46], V. Takalo[65], B. Tál[95], T. Tala[94], A.R. Talbot[3], C. Taliercio[7], P. Tamain[4], C. Tame[3], M. Tardocchi[33], L. Taroni[7], K.A. Taylor[3], G. Telesca[10], N. Teplova[41], A. Terra[29], D. Testa[23], B. Teuchner[25], S. Tholerus[31], F. Thomas[25], J.D. Thomas[3], P. Thomas[42], A. Thompson[3], C.-A. Thompson[3], V.K. Thompson[3], L. Thomson[3], L. Thorne[3], P.A. Tigwell[3], N. Tipton[3], I. Tiseanu[69], H. Tojo[43], M.Z. Tokar[29], M. Tomeš[37], P. Tonner[3], S. Tosti[74], M. Towndrow[3], P. Trimble[3], M. Tripsky[47], M. Tsalas[28], E. Tsitrone[4], D. Tskhakaya Jun[86], O. Tudisco[74], I. Turner[3], M.M. Turner[22], M. Turnyanskiy[25], G. Tvalashvili[3], S.G.J. Tyrrell[3], Z. Ul-Abidin[3], D. Ulyatt[3], B. Unterberg[29], H. Urano[43], I. Uytdenhouwen[60,]

A.P. Vadgama[3], D. Valcarcel[3,40], M. Valisa[7], M. Valovic[3], D. Van Eester[47], W. Van Renterghem[60], G.J. van Rooij[28], C.A.F. Varandas[40], S. Varoutis[44], S. Vartanian[4], K. Vasava[34], V. Vdovin[55], J. Vega[46], G. Verdoolaege[10,47], R. Verhoeven[3], C. Verona[79], M. Vervier[47], E. Veshchev[42], D. Vézinet[4], J. Vicente[40], S. Villari[74], F. Villone[84], I. Vinyar[57], B. Viola[74], R. Vitelli[79], A. Vitins[87], M. Vlad[69], I. Voitsekhovitch[3,25], P. Vondráček[37], M. Vrancken[47], W.W Pires de Sa[39], C.W.F. Waldon[3], M. Walker[3], M. Walsh[42], R.J. Warren[3], J. Waterhouse[3], N.W. Watkins[19], C. Watts[42], T. Wauters[47], M.W. Way[3], A. Webster[3], A. Weckmann[31], J. Weiland[11], H. Weisen[23], M. Weiszflog[15], S. Welte[44], J. Wendel[44], R. Wenninger[25,49], A.T. West[3], M.R. Wheatley[3], S. Whetham[3], A.M. Whitehead[3], B.D. Whitehead[3], P. Whittington[3], A.M. Widdowson[3], S. Wiesen[29], D. Wilkes[3], J. Wilkinson[3], M. Williams[3], A.R. Wilson[3], D.J. Wilson[3], H.R. Wilson[92], M. Wischmeier[49], G. Withenshaw[3], D.M. Witts[3], D. Wojciech[36], A. Wojeński[36], D. Wood[3], S. Wood[3], C. Woodley[3], U. Woźnicka[36], J. Wright[3], J. Wu[73], L. Yao[73], D. Yapp[3], V. Yavorskij[86], M.G. Yoo[62], J. Yorkshades[3], C. Young[3], D. Young[3], I.D. Young[3], W. Zabolotny[36], J. Zacks[3], R. Zagorski[36], F.S. Zaitsev[13], R. Zanino[58], V. Zaroschi[69], K.D. Zastrow[3], W. Zeidner[49], A. Ziółkowski[36], V. Zoita[69], S. Zoletnik[95], I. Zychor[36].

[1] Aalto University, P.O.Box 14100, FIN-00076 Aalto, Finland

[2] BCS, Barcelona, Spain

[3] CCFE, Culham Science Centre, Abingdon, Oxon, OX14 3DB, UK

[4] CEA, IRFM, F-13108 Saint Paul Lez Durance, France

[5] Centro Brasileiro de Pesquisas Fisicas, Rua Xavier Sigaud, 160, Rio de Janeiro CEP 22290-180, Brazil

[6] Consorzio CREATE, Via Claudio 21, 80125 Napoli, Italy

[7] Consorzio RFX, corso Stati Uniti 4, 35127 Padova, Italy

[8] Daegu University, Jillyang, Gyeongsan, Gyeongbuk 712-174, Republic of Korea

[9] Departamento de Física, Universidad Carlos III de Madrid, 28911 Leganés, Madrid, Spain

[10] Department of Applied Physics UG (Ghent University) St-Pietersnieuwstraat 41 B-9000 Ghent Belgium

[11] Department of Earth and Space Sciences, Chalmers University of Technology, SE-41296 Gothenburg, Sweden

[12] Department of Electrical and Electronic Engineering, University of Cagliari, Piazza d'Armi 09123 Cagliari, Italy

[13] Department of Experimental Physics, Faculty of Mathematics, Physics and Informatics Comenius University Mlynska dolina F2, 84248 Bratislava, Slovak Republic

[14] Department of Physics and Applied Physics, University of Strathclyde, Glasgow, G4 ONG, UK

[15] Department of Physics and Astronomy, Uppsala University, SE-75120 Uppsala, Sweden

[16] Department of Physics, Lund University, SE-22100 Lund, Sweden

[17] Department of Physics, SCI, KTH, SE-10691 Stockholm, Sweden
[18] Department of Physics, University of Oxford, OX1 2JD
[19] Department of Physics, University of Warwick, Coventry, CV4 7AL, UK
[20] Department of Pure and Applied Physics, Queens University, Belfast, BT7 1NN, UK
[21]Dipartimento di Ingegneria Elettrica Elettronica e dei Sistemi-Università degli Studi di Catania, 95125 Catania, Italy
[22] Dublin City University (DCU), Ireland
[23] Ecole Polytechnique Fédérale de Lausanne (EPFL), CRPP, CH-1015 Lausanne, Switzerland
[24] Ecole Polytechnique, CNRS UMR7648, LPP, F-91128, Palaiseau, France
[25] EUROfusion Programme Management Unit, Boltzmannstr. 2, 85748 Garching, Germany
[26] EUROfusion Programme Management Unit, Culham Science Centre, OX14 3DB Abingdon, United Kingdom
[27] European Commission, B-1049 Brussels, Belgium
[28] FOM Institute DIFFER P.O. Box 1207 NL-3430 BE Nieuwegein, The Netherlands
[29] Forschungszentrum Jülich GmbH, Institut für Energie- und Klimaforschung - Plasmaphysik, 52425 Jülich, Germany
[30] Fusion for Energy Joint Undertaking, Josep Pl. 2, Torres Diagonal Litoral B3, 08019, Barcelona, Spain
[31] Fusion Plasma Physics, EES, KTH, SE-10044 Stockholm, Sweden
[32] General Atomics, P.O.Box 85608, San Diego, CA 92186-5608, California, USA
[33] IFP-CNR, via R. Cozzi 53, 20125 Milano, Italy
[34] Institute for Plasma Research, Bhat, Gandhinagar - 382 428, Gujarat State, India
[35] Institute of Electronics, Bulgarian Academy of Sciences, 72 Tzarigradsko shosse, Sofia 1784, Bulgaria
[36] Institute of Plasma Physics and laser Microfusion, Hery 23, 01-497 Warsaw, Poland
[37] Institute of Plasma Physics AS CR, Za Slovankou 1782/3, 182 00 Praha 8, Czech Republic
[38] Institute of Plasma Physics, Chinese Academy of Sciences, Hefei, 230031, China
[39] Instituto de Física - Universidade de São Paulo Rua do Matão Travessa R Nr.187 CEP 05508-090 Cidade Universitária, São Paulo - Brasil
[40] Instituto de Plasmas e Fusão Nuclear, Instituto Superior Técnico, Universidade de Lisboa, Portugal
[41] Ioffe Physico-Technical Institute, 26 Politekhnicheskaya, St Petersburg 194021, Russian Federation
[42] ITER Organization, Route de Vinon, CS 90 046, 13067 Saint Paul Lez Durance, France
[43] Japan Atomic Energy Agency, Naka Fusion Research Establishment, Nakamachi, Nakagun, Ibaraki-ken 311-0913, Japan,44 Karlsruhe Institute of Technology, P.O.Box 3640, D-76021 Karlsruhe, Germany
[45] Laboratoire J.A.Dieudonné, Université de Nice-Sophia-Antipolis, Parc Valrose, F-06108 Nice CEDEX 02, France

[46] Laboratorio Nacional de Fusión, CIEMAT, Madrid, Spain
[47] Laboratory for Plasma Physics Koninklijke Militaire School - Ecole Royale Militaire Renaissancelaan 30 Avenue de la Renaissance B-1000, Brussels, Belgium
[48] Lithuanian energy institute, Breslaujos g. 3, LT-44403, Kaunas, Lithuania
[49] Max-Planck-Institut für Plasmaphysik, D-85748 Garching, Germany
[50] Max-Planck-Institut für Plasmaphysik, Teilinsitut Greifswald, D-17491 Greifswald Germany
[51] MIT Plasma Science and Fusion Centre, Cambridge, MA 02139, Massachusetts, USA
[52] National Fusion Research Institute(NFRI) 169-148 Gwahak-ro, Yuseong-gu, Daejeon 305- 806, Korea
[53] National Technical University of Athens, Iroon Politechniou 9, 157 73 Zografou, Athens, Greece
[54] NCSR "Demokritos" 153 10, Agia Paraskevi Attikis, Greece
[55] NRC Kurchatov Institute, 1 Kurchatov Square, Moscow 123182, Russian Federation
[56] Oak Ridge National Laboratory, Oak Ridge, TN 37831-6169, Tennessee, USA
[57] PELIN LLC, 27a, Gzhatskaya Ulitsa, Saint Petersburg, 195220, Russia
[58] Politecnico di Torino, Corso Duca degli Abruzzi 24, I-10129 Torino, Italy
[59] Princeton Plasma Physics Laboratory, James Forrestal Campus, Princeton, NJ 08543, New Jersey, USA
[60] SCK-CEN, Nuclear Research Centre, 2400 Mol, Belgium
[61] Second University of Napoli, Consorzio CREATE, Via Claudio 21, 80125 Napoli, Italy
[62] Seoul National University, Shilim-Dong, Gwanak-Gu, Republic of Korea
[63] Slovenian Fusion Association (SFA), Jozef Stefan Institute, Reactor Physics Department, Jamova 39, SI-1000 Ljubljana, Slovenia
[64] Switzerland - Department of Physics, University of Basel
[65] Tampere University of Technology, P.O. Box 527, FI-33101 Tampere, Finland
[66] Technical University of Denmark, Department of Physics, Bldg 309, DK-2800 Kgs Lyngby, Denmark
[67] The "Horia Hulubei" National Institute for Physics and Nuclear Engineering, Magurele-Bucharest, Romania
[68] The National Institute for Cryogenics and Isotopic Technology, Ramnicu Valcea, Romania
[69] The National Institute for Laser, Plasma and Radiation Physics, Magurele-Bucharest, Romania
[70] The National Institute for Optoelectronics, Magurele-Bucharest, Romania
[71] The Nuclear Fuel Plant, Pitesti, Romania
[72] Troitsk Insitute of Innovating and Thermonuclear Research (TRINITI), Troitsk 142190, Moscow Region, Russian Federation
[73] Uni of Electronic Science & Tech of China
[74] Unità Tecnica Fusione - ENEA C. R. Frascati - via E. Fermi 45, 00044 Frascati (Roma), Italy
[75] Universidad Complutense de Madrid, Madrid, Spain
[76]Universidad de Sevilla, Sevilla, Spain

[77]Universidad Nacional de Educación a Distancia, Madrid, Spain,
[78]Universidad Politécnica de Madrid, Grupo I2A2, Madrid, Spain
[79]Università di Roma, Italy
[80]University College Cork (UCC), Ireland,
[81]University Milano-Bicocca, piazza della Scienza 3, 20126 Milano, Italy,
[82]University of Basilicata, Consorzio CREATE, Via Claudio 21, 80125 Napoli, Italy,
[83]University of California, 1111 Franklin St., Oakland, CA 94607, USA,
[84]University of Cassino, Consorzio CREATE, Via Claudio 21, 80125 Napoli, Italy,
[85] University of Helsinki, P.O. Box 43, FI-00014 University of Helsinki, Finland
[86] University of Innsbruck, Fusion@Österreichische Akademie der Wissenschaften (ÖAW), Austria
[87] University of Latvia, 19 Raina Blvd., Riga, LV 1586, Latvia
[88] University of Napoli "Federico II", Consorzio CREATE, Via Claudio 21, 80125 Napoli, Italy
[89] University of Napoli Parthenope, Consorzio CREATE, Via Claudio 21, 80125 Napoli, Italy
[90] University of Tartu, Ülikooli 18, 50090 Tartu, Estonia
[91] University of Texas at Austin, Institute for Fusion Studies, Austin, TX 78712, Texas, USA
[92] University of York, Heslington, York YO10 5DD, UK
[93] Vienna University of Technology, Fusion@Österreichische Akademie der Wissenschaften (ÖAW), Austria
[94] VTT Technical Research Centre of Finland, P.O.Box 1000, FIN-02044 VTT, Finland
[95] Wigner Research Centre for Physics, P.O.B. 49, H - 1525 Budapest, Hungary